Theriogenology 250 (2026) 117711

Contents lists available at ScienceDirect

Theriogenology

journal homepage: www.theriojournal.com

Original Research Article

Nanoplastics internalization impairs mitochondrial activity in equine sperm

Sofia Dindo [a], Laura Tovar-Pascual [a], Vito Antonio Baldassarro [a], Diego Bucci [a], Beatrice Mislei [a,b], Marcella Spinaci [a], Jose Manuel Ortiz-Rodriguez [a,*]

[a] Department of Veterinary Medical Sciences, Alma Mater Studiorum-University of Bologna, Via Tolara di Sopra 50, Ozzano dell'Emilia, Bologna, 40064, Italy
[b] National Institute of Artificial Insemination (AUB-INFA), University of Bologna, Via Gandolfi 16, Cadriano, Bologna, 40057, Italy

ARTICLE INFO

Keywords:
Spermatozoa
Nanoplastics
Plastic pollution
Mitochondria
Oxidative stress
Fertility
Equine

ABSTRACT

Nanoplastics (NP) accumulation in biological tissues and their adverse effects on fertility through inflammatory and oxidative stress responses have recently been described as consequences of global plastic pollution. However, little is known about the impact of NP on gametes. This study aimed to assess the internalization of NP and their effects on mature equine spermatozoa. Frozen-thawed ejaculates from five stallions were divided into untreated control (CTR) and samples supplemented with different concentrations (10, 50, 100 and 200 μg/mL) of 30 nm polystyrene NP. At baseline (T0), and after 1 (T1) and 3 h (T3) of incubation at 38 °C, sperm viability, mitochondrial activity, and intracellular ROS were evaluated by flow cytometry, while sperm motility was assessed using a CASA system. NP internalization was analyzed by confocal microscopy and flow cytometry using fluorescent NP. Results showed that NP were internalized by live spermatozoa, accumulating in the post-acrosomal and/or the mid piece region. NP exposure led to reduced sperm viability (CTR T1: 50.7 ± 14.0 % vs 200 μg/mL T1: 36.6 ± 11.8 %, $p < 0.05$), decreased mitochondrial activity (CTR T1: 35.4 ± 15.8 % vs 200 μg/mL T1: 16.3 ± 14.0 %, $p < 0.001$), and increase proportions of live sperm with high intracellular $O_2^{-}\cdot$ levels (CTR T1: 39.0 ± 10.1 % vs 200 μg/mL T1: 47.3 ± 11.0 %, $p < 0.05$). These results allow us to conclude that equine sperm quality may be compromised by nanoplastics internalization, which pre-eminently impairs mitochondrial activity. This research furnishes some bases for further studies on the potential implications of NP exposure for fertility.

1. Introduction

The current global plastic pollution is one of the main emerging threats for human and environmental health. The principal consequence of the presence of plastics from human activities in all ecosystems worldwide is the dissemination of particles derived from large plastic fractions or laboratory-synthesized polymers, especially used as additives in personal care products, pharmaceutical carriers, and the production of synthetic textiles. Plastic particles with a diameter minor than 5 mm are called microplastics (MP), which can be derived into nanoplastics (NP), plastic fragments with a diameter of 1–100 nm, by biological, physical, or chemical disaggregation [1–3]. The most common types of MP include long-lasting synthetic compounds as polyethylene, polypropylene, polystyrene, polyvinyl chloride, and polyethylene terephthalate [1,2].

Humans and animals can internalize MP and NP (MNP) by ingestion, inhalation and dermal contact, as MNP have been identified in different food substances, water sources and in the atmosphere [4–6]. Several studies have shown the accumulation of plastic particles in human and animals' tissues [7,8], posing a potential health risk due to inflammatory effects and altered biomarkers indicative of toxicity [9–11]. Recently, in vitro cell culture studies and in vivo experiments in laboratory animals reported that exposure to MNP may affect multiple human organ systems by inducing oxidative stress, inflammation, immune dysfunction, alterations in biochemical and energy metabolism, impaired cell proliferation, disruption of microbial metabolic pathways, and potential carcinogenicity [6,12–18]. The effects of MNP accumulation vary depending on their composition, size, and concentration within tissues. Due to their smaller size and greater cellular affinity, NP can bypass biological barriers, enter the bloodstream, and reach cells, tissues, and organs, potentially posing a higher risk than MP [2,3]. Although research is still emerging, growing evidence indicates that NP may exert endocrine-disrupting effects on metabolic and reproductive health by penetrating cells and interacting with molecular targets [4]. Regarding the reproductive system, several studies report adverse effects of MNP on mouse testis following oral exposure to polystyrene MP. These

* Corresponding author. Via Tolara di Sopra 50, Ozzano dell'Emilia, Bologna, 40064, Italy.
E-mail address: jose.ortiz@unibo.it (J.M. Ortiz-Rodriguez).

https://doi.org/10.1016/j.theriogenology.2025.117711
Received 27 June 2025; Received in revised form 17 September 2025; Accepted 13 October 2025
Available online 14 October 2025

include structural damage, disruption of blood–testis barrier, inflammation, impaired spermatogenesis, and increased sperm abnormalities [19–22]. The accumulation of NP within testicular tissues is hypothesized to contribute to the global deterioration of human semen quality, acting synergistically with environmental factors such as heavy metal exposure [8,23]. The incubation of mature human spermatozoa with NP has been associated with increased acrosomal damage, elevated oxidative stress marked by reactive oxygen species (ROS) generation, DNA fragmentation, and impaired mitochondrial activity [24].

Current knowledge regarding the impact of MNP on mammals' male gametes and on their reproductive performance remains limited. In this regard, the present study aimed to investigate the internalization rate and the effects of NP on stallion mature spermatozoa.

2. Materials and Methods

2.1. Chemicals and reagents

Unless otherwise specified, all chemicals and reagents were purchased from Sigma-Aldrich (Milan, Italy). Polystyrene microspheres with a diameter of 0.03 μm, Hoechst 33342, CM-H2DCFDA, DRAQ7™ Dye, SYTOX™ Green Nucleic Acid Stain, Dihydroethidium (DHE), JC-1 Dye, and Vybrant™ Dil Cell-Labeling Solution were purchased from Invitrogen (Thermo Fisher Scientific, Waltham, MA, USA). Zombie Violet™ Fixable Viability Kit was purchased from BioLegend (San Diego, CA, United States). VECTASHIELD® Antifade Mounting Medium was purchased from Vector Laboratories, Inc., (Newark, CA, USA).

2.2. Semen processing

Fifteen frozen ejaculates from five fertile stallions were obtained from the National Institute for Artificial Insemination (AUB-INFA, University of Bologna, Italy), with three ejaculates collected per stallion. Before and after freezing, AUB-INFA evaluated the semen for morphology, concentration, and motility according to the center's standard protocol. The fertility of the ejaculates was also confirmed, ensuring their suitability for the present study.

Semen straws were thawed in a water bath at 37 °C for at least 30 s and diluted (1:4) in pre-warmed modified Biggers Whitten and Whittingham medium (BWW), containing 95 mM NaCl, 4.7 mM KCl, 1.7 mM $CaCl_2.2H_2O$, 1.2 mM KH_2PO_4, 1.2 mM $MgSO_4.7H_2O$, 25 mM $NaHCO_3$, 5.6 mM D-Glucose, 275 μM $C_3H_3NaO_3$, 3.7 μL/mL 60 % $NaC_3H_5O_3$ syrup, 50 U/mL penicillin, 50 μg/mL streptomycin, 20 mM HEPES, and 0.1 % (w/v) polyvinyl alcohol (PVA), with an osmolarity of approximately 310 mOsm/kg and a pH of 7.4. Samples were washed once by centrifugation at 600*g* for 3 min and resuspended in BWW to obtain a final concentration of 60×10^6 spermatozoa/mL.

2.3. Experimental design

2.3.1. Experiment 1: effects of NP exposure on mature equine spermatozoa

Two working solutions of 30 nm polystyrene nanoplastics (Thermo Fisher Scientific, Cat. No. 5003A) were prepared in BWW medium (NP; 0.2 and 5 mg/mL) and sonicated for 4 min using a MISONIX sonicator to prevent NP aggregation. Semen aliquots (three replicates per stallion, n = 15) were adjusted to a concentration of 30×10^6 spermatozoa/mL and incubated at 38 °C for 3 h either without (control, CTR) or with NP at concentrations of 10, 50, 100 or 200 μg/mL (10NP, 50NP, 100NP and 200NP, respectively). The concentrations and diameter of the NP used in this study were determined based on a combination of literature-based evidence and preliminary experimental trials. Initial reference points were drawn from previous in vitro studies involving the incubation of human spermatozoa with NP [24], assessments of NP concentrations ranging from 20 to 100 μm in the semen and testes of humans and dogs [8,23], and in vitro studies on oocytes exposed to NP [25]. Additionally, a recent study described the presence of polystyrene NP, among others, in drinking water at concentration ranging from 60 to 530 μg/mL [26]. Preliminary trials were then conducted to refine these concentrations and construct a sperm survival curve.

Assessments were conducted immediately after thawing (T0, CTR group) and after 1 h (T1) and 3 h (T3) of incubation in all groups. Sperm kinetic parameters were evaluated using a Computer-Assisted Sperm Analysis (CASA) system, and sperm viability, mitochondrial activity, and reactive oxygen species (ROS) production were assessed by flow cytometry, as described below.

2.3.2. Experiment 2: evaluation of NP internalization in mature equine spermatozoa

Given that the results of Experiment 1 showed an effect of NP on sperm viability, mitochondrial activity, and ROS production, Experiment 2 was designed to evaluate NP internalization using 30 nm fluorescent yellow-green ($\lambda_{ex} \sim 470$ nm; $\lambda_{em} \sim 505$ nm) carboxylate-modified polystyrene beads (Fluo-NP; Sigma-Aldrich, Cat. No. L5155).

Two working solutions of Fluo-NP (0.2 and 5 mg/mL) were prepared in BWW medium and sonicated for 4 min using a MISONIX sonicator to prevent NP aggregation. Semen aliquots (one replicate per stallion, n = 5) were adjusted to a concentration of 30×10^6 spermatozoa/mL and incubated at 38 °C either without (control, CTR) or with Fluo-NP at concentrations of 10, 50, 100 or 200 μg/mL (referred to as 10NP, 50NP, 100NP and 200NP, respectively).

Assessments were performed after 1 h (T1) of incubation using flow cytometry for all experimental groups and replicates, while confocal microscopy was conducted only for the CTR and 100NP groups in one selected replicate, as described below.

2.4. Computer-assisted sperm analysis (CASA)

Sperm kinetic parameters were assessed with a computer-assisted sperm analysis (CASA) system (AiStation, SPERM.TECH®, Sperm Analysis Technologies, Valencia, Spain), equipped with a monochrome camera (Basler Ace 2048x1536, 120 fps, mono 2/3″ IMX252, CMOS, Global shutter, C-Mount, USB3 Vision) mounted on a phase-contrast microscope (Nikon Eclipse E400) with 10× magnification. A 5 μL aliquot of each sample was placed in a pre-warmed (38 °C) Spermtrack 20 chamber (Proiser R + D S.L., Paterna, Spain), and a minimum of 500 spermatozoa per sample were evaluated across at least five randomly selected fields. Spermatozoa with an average path velocity (VAP) > 30 μm/s were considered motile, and a straightness (STR) threshold of 75 % was used to classify sperm as progressive.

2.5. Flow cytometry analysis

Flow cytometry analyses were performed using a CytoFLEX® S flow cytometer (Beckman Coulter) equipped with three lasers (405 nm, 488 nm, and 561 nm). The instrument was calibrated daily using specific calibration beads provided by the manufacturer, and spectral overlap compensation was carried out prior to each experiment. Unstained and single-stained controls were used to establish compensation settings and thresholds for distinguishing positive from negative events, as well as to define regions of interest for different dyes.

Sperm subpopulations were categorized into quadrants to quantify the frequency of each subset. Side scatter height (SSC-H) and forward scatter height (FSC-H) were recorded in logarithmic mode (FSC vs. SSC dot plots) for a total of 10000 events per sample. Non-sperm events were excluded by gating the sperm population based on Hoechst 33342 staining, a cell-permeable DNA stain emitting blue fluorescence at 486 nm. All Hoechst 33342-positive events within a specific side scatter (SCC) range were considered spermatozoa.

For each assay, sperm concentration was adjusted to 2.5×10^6 spermatozoa/mL in a final volume of 250 μL of BWW, and cells were stained with the appropriate combinations of fluorochromes, as described below. Signals were logarithmically amplified, and

photomultiplier settings were optimized according to each staining protocol. Data were acquired using CytExpert Acquisition Software (Beckman Coulter), exported as FCS files, and subsequently analyzed with FlowJo v10.10 software (BD (Becton, Dickinson & Company) Ashland, OR, USA).

2.5.1. Sperm viability and mitochondrial membrane potential

Sperm aliquots were stained with 3 μM Hoechst 33342 to identify spermatozoa, 1.5 μM DRAQ7 to evaluate sperm viability, and 2 μM JC-1 to assess mitochondrial membrane potential, and incubated at 37 °C for 30 min in the dark.

DRAQ7 is a membrane-impermeable dye that stains double-stranded DNA (dsDNA) of dead or permeabilized cells, with maximum emission at 697 nm. JC-1 is a potential-sensitive carbocyanine dye that accumulates in mitochondria, shifting fluorescence from green (525 nm) at low membrane potential (monomeric form) to orange (590 nm) at high membrane potential (J-aggregates). Mitochondrial depolarization is indicated by a decrease in the orange/green fluorescence intensity ratio. Therefore, mitochondria with high membrane potential (HMP) emit predominantly orange fluorescence, while those with low mitochondrial membrane potential (LMP) emit green fluorescence. The percentage of live spermatozoa (DRAQ7-negative) with HMP (JC-1 orange fluorescence) was quantified in all samples.

2.5.2. Superoxide ($O_2^{-}\cdot$) in live sperm

Sperm aliquots were stained with 3 μM Hoechst 33342 to identify spermatozoa, 60 nM SYTOX Green to evaluate viability, and 2 μM DHE to assess intracellular $O_2^{-}\cdot$ levels, and incubated at 37 °C for 15 min in the dark.

SYTOX Green is a cell-impermeant nucleic acid stain that labels non-viable cells, emitting at 525 nm. DHE is a superoxide indicator that emits bright fluorescent red at 582 nm. The percentage of live spermatozoa (SYTOX Green-negative) with high intracellular $O_2^{-}\cdot$ levels (DHE-positive) was quantified in all samples.

2.5.3. Hydrogen peroxide (H_2O_2) in live sperm

Sperm aliquots were stained with 3 μM Hoechst 33342 to identify spermatozoa, 12 nM propidium iodide (PI) to evaluate viability, and 5 μM CM-H_2DCFDA to assess intracellular H_2O_2 levels, and incubated at 37 °C for 20 min in the dark.

PI is a membrane-impermeable dye that stains the nuclei of non-viable cells, emitting red fluorescence at 620 nm. CM-H_2DCFDA is a chloromethyl derivative of H_2DCFDA, used as an indicator for reactive oxygen species (ROS), particularly H_2O_2, with emission at 517–527 nm. The median fluorescence intensity (MFI) of the 525 nm emission in the live sperm population (PI-negative) was quantified in all samples to determine intracellular H_2O_2 levels.

2.5.4. NP internalization in spermatozoa

Sperm aliquots from the different groups in Experiment 2 were stained with 3 μM Hoechst 33342 to identify spermatozoa and 1.5 μM DRAQ7 to assess viability. Samples were incubated at 37 °C for 20 min in the dark.

As indicated above, DRAQ7 stains non-viable sperm and emits at 697 nm. Fluorescent yellow-green NP were detected via their emission at 525 nm. The median fluorescence intensity (MFI) at 525 nm within the live sperm population (DRAQ7-negative) was quantified in all samples to evaluate intracellular NP levels.

2.6. Confocal microscopy

After 1 h of incubation, sperm aliquots from the CTR and 100NP groups (one replicate from Experiment 2) were stained with Zombie Violet (1:1000 dilution), a fixable viability dye, and incubated at 37 °C for 30 min in the dark. Samples were then centrifuged at 900 g for 2 min and washed with PBS. Following washing, sperm were resuspended in 100 μL of PBS containing 2 % paraformaldehyde and incubated for 5 min at 4 °C. After fixation, samples were centrifuged again and washed in PBS. The resulting pellet was resuspended in PBS containing 5 μM Vybrant DiI and incubated for 30 min at 37 °C. After a final centrifugation and wash step, cells were resuspended in 30 μL of PBS. A 10 μL drop of each sample was placed on a microscope slide, air-dried, and mounted with VECTASHIELD mounting medium. Slides were covered with 22 × 22 mm coverslips and stored protected from light until imaging.

Zombie Violet is an amine-reactive fluorescent dye that is non-permeant to live cells but can enter cells with compromised membranes, emitting violet fluorescence with a peak at 423 nm in non-viable spermatozoa. Vybrant DiI is a lipophilic membrane dye with peak emission at 665 nm and is used to label sperm membranes. As previously described, fluorescent yellow-green nanoplastics (NP) emit fluorescence at 525 nm.

In this assay, live spermatozoa (Zombie Violet-negative) were identified, and the membrane was labeled with Vybrant DiI, enabling assessment of NP localization within the spatial boundaries of the sperm cell.

Imaging was performed using a Nikon Ti-E fluorescence microscope, connected to an A1R confocal system (Nikon, Minato, Tokyo, Japan). Images (1024 × 1024 pixels resolution) were acquired using a 40 × and a 60× objective implemented with a 3× digital zoom. All z-stacks were collected in compliance with the optical section separation values indicated by the acquisition software (NIS-Element AR 3.2; 0.5 μm; 14–15 images). To obtain the best signal-to-noise ratio, an average of 2 acquisition per image was performed. Images were elaborated using a voxel-based software (IMARIS, v. 9.7.2; Oxford Instruments plc, Tubney Woods, Abingdon, Oxon, UK). Using the "surface" algorithm, the isosurfaces of the fluorescence was reconstructed to generate the volume occupied by both the cell and the NP.

2.7. Statistical analysis

Data were analyzed using the R v. 4.4.3. (R Foundation for Statistical Computing, Vienna, Austria). Unless otherwise specified, results are presented as the mean ± SD and the level of significance used was $p \leq 0.05$. The Shapiro-Wilk test was used to assess normality. Linear mixed-effects models were used to assess the fixed effect of treatment, incubation time, and their interaction, including stallion and ejaculate as random effects. Tukey post-hoc test was subsequently run to determine differences between groups.

3. Results

3.1. Mature stallion spermatozoa internalize nanoplastics

A rightward shift in fluorescence intensity in live spermatozoa was observed after 1 h of incubation, corresponding to increasing Fluo-NP concentration (Fig. 1). Confocal microscopy confirmed NP internalization in live spermatozoa, with marked accumulation in the post-acrosomal region and/or the mid piece (Fig. 2).

3.2. NP impair sperm viability

NP internalization led to a decrease in sperm survival during incubation. The highest NP concentration caused a reduction in viability after 1 h (CTR: 50.7 ± 14.0 % vs 200NP: 36.6 ± 11.8 %, $p < 0.05$). A decrease was also observed in the 100 μg/mL group after 3 h (CTR: 49.3 ± 11.8 % vs 100NP: 44.0 ± 11.2 %, $p < 0.05$). Furthermore, only the highest concentration showed a decline in viability between T1 and T3 (200NP T1: 36.6 ± 11.8 % vs 200NP T3: 27.0 ± 7.1 %, $p < 0.05$) (Fig. 3).

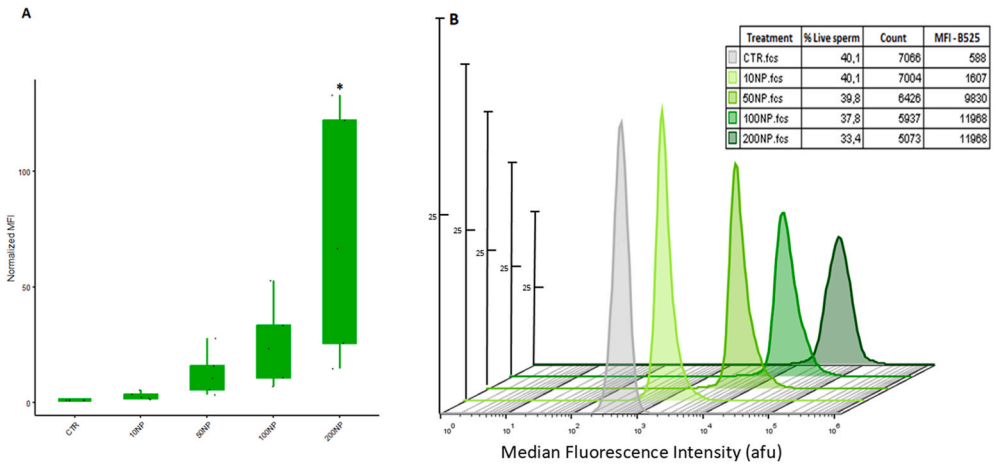

Fig. 1. Internalization of nanoplastics (NP) in stallion spermatozoa was assessed using 30 nm green fluorescent NP. As described in the Materials and Methods section, frozen-thawed semen aliquots were incubated 1 h at 38 °C either without (CTR) or with fluorescent NP at 10, 50, 100 or 200 μg/mL (10NP, 50NP, 100NP and 200NP, respectively). NP internalization was evaluated as the median fluorescence intensity (MFI) in the live spermatozoa population. **(A)** Histogram showing the MFI for each assay, with individuals points representing each replicate (n = 5) and whiskers indicating SD. Values were normalized to the corresponding CTR within each experiment, allowing comparison of relative increases in fluorescence. A concentration-dependent increase in MFI is observed, and an asterisk indicates a statistically significant difference ($p < 0.05$). **(B)** Representative overlay of flow cytometry histograms showing green fluorescence intensity in the live sperm population from one replicate. A rightward shift in fluorescence intensity is observed with increasing NP concentrations, indicating higher internalization. Additionally, a decrease in histogram peak height (Count) is evident, reflecting a reduced number of live spermatozoa. This reduction corresponds to a decrease in sperm viability percentage (% Live sperm) with higher NP exposure. (For interpretation of the references to colour in this figure legend, the reader is referred to the Web version of this article.)

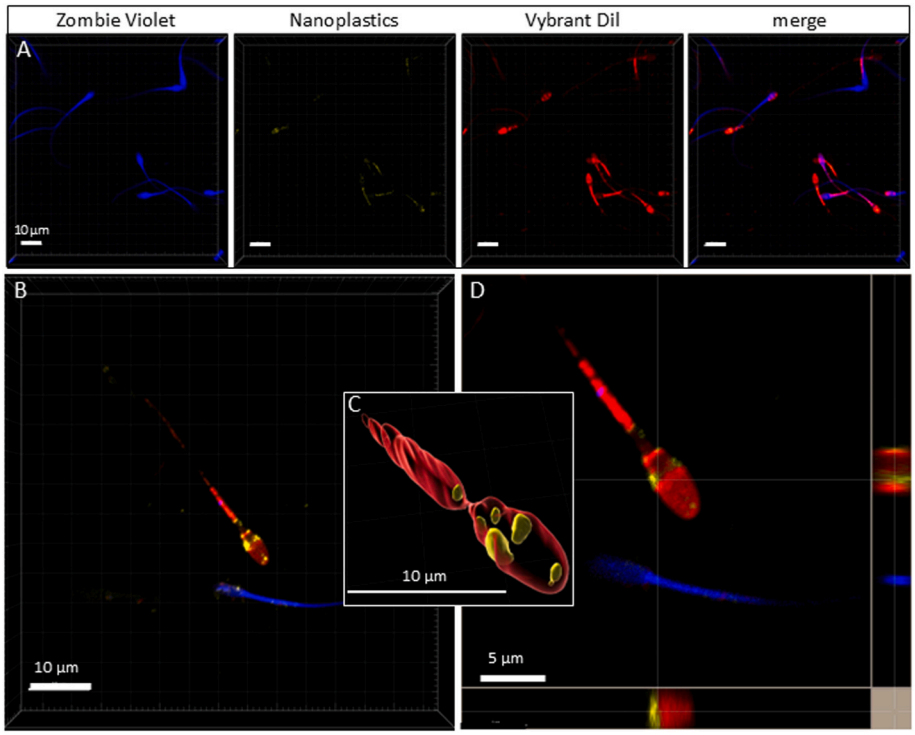

Fig. 2. Representative images of internalization and localization of nanoplastics (NP) in live spermatozoa. Sperm were incubated for 1 h at 38 °C with 100 μg/mL fluorescent NP (yellow), and stained with Zombie Violet (blue, dead sperm) and Vybrant DiI (red, membrane marker). **(A)** Z-stacks acquired by confocal microscopy and processed with IMARIS voxel-based software (40 × objective, 3 × digital zoom). **(B)** Higher magnification images (60 × objective, 3 × digital zoom) showing a dead sperm (blue) and a single live sperm (red). **(C)** 3D reconstruction of the head and midpiece (red) from a live spermatozoon, with NP localization (yellow) using the isosurface rendering. **(D)** Projections of the z-stack images in which it is possible to recognize the NP (yellow) inside the live sperm (red). (For interpretation of the references to colour in this figure legend, the reader is referred to the Web version of this article.)

3.3. NP reduce mitochondrial activity in live spermatozoa and increase intracellular superoxide levels

In addition to reduced viability, NP supplementation decreased mitochondrial activity in the live sperm population. The percentage of live sperm with high mitochondrial membrane potential (HMP) was lower in the two highest concentration groups after 1 h of incubation (CTR: 35.4 ± 15.8 % vs 100NP: 28.0 ± 17.2 %, $p < 0.05$; and CTR vs

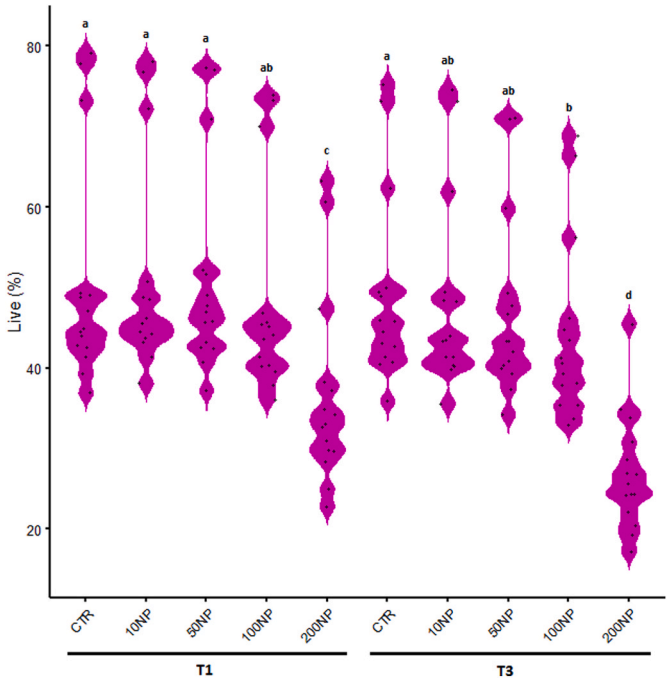

Fig. 3. Effect of NP supplementation on stallion spermatozoa viability. As described in the Materials and Methods section, frozen-thawed semen aliquots were incubated at 38 °C either without (CTR) or with 30 nm polystyrene nanoplastics at 10, 50, 100 or 200 μg/mL (10NP, 50NP, 100NP and 200NP, respectively). Sperm viability, assessed as the percentage of live spermatozoa, was evaluated after 1 h (T1) and 3 h (T3) of incubation. Data distribution is visualized using violin plots generated in R, displaying kernel density estimation and individual data points. Different letters indicate statistically significant differences between treatment-time combinations ($p < 0.001$), supported by a significant interaction effect in the two-way ANOVA.

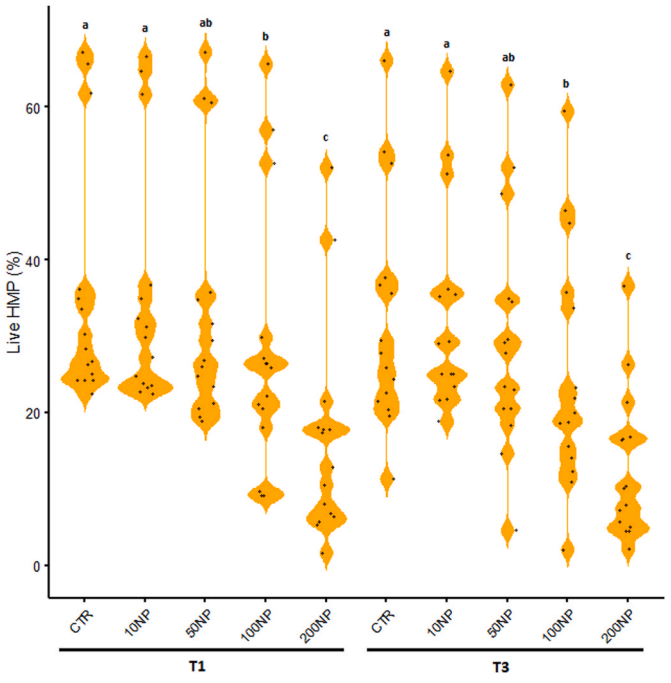

Fig. 4. Effect of NP supplementation on stallion spermatozoa mitochondrial activity. As described in the Materials and Methods section, frozen-thawed semen aliquots were incubated at 38 °C either without (CTR) or with 30 nm polystyrene nanoplastics at 10, 50, 100 or 200 μg/mL (10NP, 50NP, 100NP and 200NP, respectively). Mitochondrial activity, assessed as the percentage of live spermatozoa with high mitochondrial membrane potential, was evaluated after 1 h (T1) and 3 h (T3) of incubation. Data distribution is visualized using violin plots generated in R, displaying kernel density estimations and individual data points. Different letters indicate statistically significant differences between treatments within the same time point ($p < 0.05$; $p < 0.001$ for 200NP treatment), in line with the absence of significant treatment-time interaction in the two-way ANOVA.

200NP: 16.3 ± 14.0 %, $p < 0.001$), and this effect persisted after 3 h (CTR: 32.4 ± 15.1 % vs 100NP: 25.2 ± 15.7 %, $p < 0.05$; and CTR vs 200NP: 12.8 ± 9.6 %, $p < 0.001$) (Fig. 4). Meanwhile, intracellular H_2O_2 levels in live sperm showed no significant changes due to NP exposure. However, the percentage of live sperm with high intracellular $O_2^{\cdot-}$ levels increased in 200NP group compared to CTR at both T1 (CTR: 39.0 ± 10.1 % vs 200NP: 47.3 ± 11.0 %, $p < 0.05$) and T3 (CTR: 38.8 ± 13.1 % vs 200NP: 55.9 ± 16.7 %, $p < 0.05$) (Fig. 5).

3.4. NP internalization affects sperm motility

Regarding sperm kinematic parameters, the highest NP concentration negatively affected spermatozoa once again, specifically by reducing total and progressive motility. However, no significant differences in velocity or trajectory parameters (VCL, VAP, VSL, STR, and LIN) were observed among the experimental groups after 1 h of incubation with NP. After 3 h, only VSL, STR, and LIN decreased with the highest NP concentration (Table 1).

4. Discussion

Plastic pollution is a growing global concern due to its potential effects on both human and animal health. The World Health Organization (WHO) has recently highlighted that knowledge about the impact of MNP remains limited, and that emerging evidence warrants urgent and systematic research (https://www.who.int/publications/i/item/9789240054608). Consequently, studies on the effects of NP have begun to emerge in both human and laboratory animal models, evidencing detrimental consequences on tissues including oxidative stress and inflammation [6,12–18]. Recent studies have shown that NP are capable of disseminating throughout the body and accumulating in various tissues and cells, which may pose potential health risks [7,9,10]. Focusing on reproductive organs, the accumulation of MNP has been identified in the testes of humans, dogs, and mice [8,23,27]. The exposure of testis cells and gametes with NP induce male reproductive dysfunctions, which include testicular inflammation and the disruption of blood-testis barrier, associated with a decrease in sperm quality [19–22]. Most available data focus on reproductive system via in vivo models, while in vitro studies at the cellular level are still limited. Given the detection of NP in human semen and their potential link to the increasing rates of infertility observed in recent years [8], it is plausible to hypothesize that such particles may also be present in the semen of other mammalian species, potentially affecting reproductive performance. For this reason, the aim of this study was to explore if NP interact with equine mature spermatozoa using an in vitro approach to further investigate their impact on male fertility. To our knowledge, this is the first study to demonstrate NP internalization in live mature spermatozoa, revealing a dose-dependent increase. Although the mechanism of internalization remains unknown, it is supposed to differ through endocytosis, as small fragments with diameters of up to 60 nm are likely to penetrate cells and reach various organelles [28]. Due to their diminutive size (30 nm), these particles can potentially reach the nucleus and mitochondria, thereby increasing the likelihood of cellular damage compared to larger particles [4,24]. The internalization of NP with a diameter of 50 nm and 500 nm across model cell membranes has also been observed, through both active endocytic pathways passive membrane diffusion facilitated by hydrophobic interactions and van der Waals forces [29].

A marked decrease in sperm survival was observed with increasing

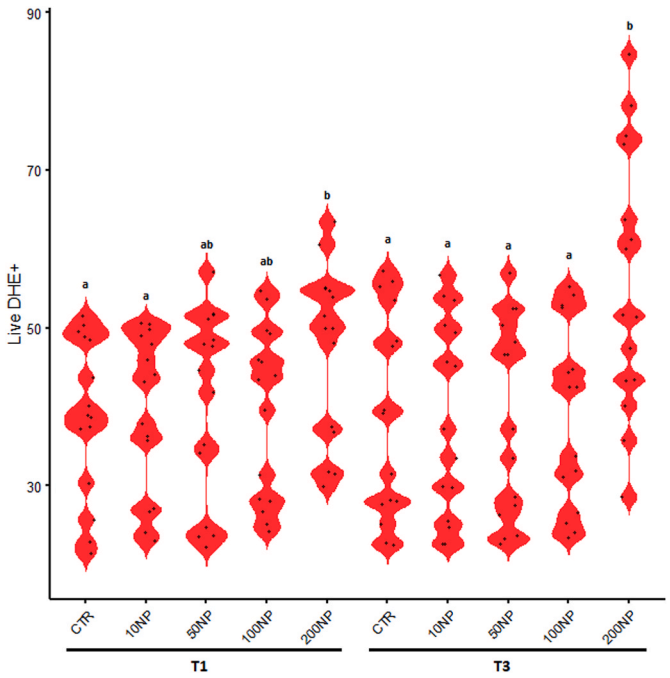

Fig. 5. Effect of NP supplementation on superoxide production by stallion spermatozoa. As described in the Materials and Methods section, frozen-thawed semen aliquots were incubated at 38 °C either without (CTR) or with 30 nm polystyrene nanoplastics at 10, 50, 100 or 200 μg/mL (10NP, 50NP, 100NP and 200NP, respectively). ROS production, assessed as the percentage of live spermatozoa with high intracellular $O_2^{-}\cdot$ levels measured by DHE staining, was evaluated after 1 h (T1) and 3 h (T3) of incubation. Data distribution is visualized using violin plots generated in R, displaying kernel density estimations and individual data points. Different letters indicate statistically significant differences between treatments within the same time point ($p < 0.05$ for T1; $p < 0.001$ for T3), consistent with the absence of significant treatment-time interaction in the two-way ANOVA.

NP concentrations, showing a synergistic effect over time that led to a further decline in viability as the incubation period progressed. This finding aligns with previous in vivo results in mice, where a significant decrease in the number of viable epididymal sperm was reported following a 35-day oral administration of 5 μm MP via drinking water. That study also reported disrupted spermatogenesis, associated with increased expression of inflammatory markers in testicular tissue [20]. Additionally, a decrease in sperm quality has been described after oral exposure to 50 nm NP, attributed to the cytotoxic effects of these particles on mouse spermatocyte, as demonstrated through in vitro evaluation [27]. In addition, internalization of NP within the cytoplasm of germ cell-derived spermatocytes (GC-sp) induces mitochondrial damage and increases apoptosis mediated by reactive oxygen species (ROS) [30], along with morphological alterations characteristic of ferroptosis [27]. In line with this evidence, our results also showed that increased NP internalization is associated with a significant decrease in the percentage of live sperm exhibiting high mitochondrial membrane potential. This effect may be related to the significant accumulation of NP in the post-acrosomal region and in the sperm midpiece where mitochondria are located, as observed by confocal microscopy (Fig. 2), [31]. Such accumulation may be driven by a combination of factors, including the particles' affinity for hydrophobic residues, the high cholesterol content, and the substantial sperm membrane plasticity [32]. Also, given their small size, mitochondrial internalization of NP could be presumed. Notably, the decrease in mitochondrial activity was accompanied by an accumulation of intracellular superoxide ($O_2^{-}\cdot$) in the population of live spermatozoa from samples exposed to high NP concentrations. It is important to highlight that $O_2^{-}\cdot$ production occurs mainly in the internal mitochondrial membrane, specifically at complexes I and III of the electron transport chain (ETC), where oxidative phosphorylation (OXPHOS) leads ATP synthesis. The $O_2^{-}\cdot$ produced by complex III is released into the intermembrane space and is converted into hydrogen peroxide (H_2O_2), which can then diffuse into the cytoplasm. In contrast, the $O_2^{-}\cdot$ generated by complex I is released directly into the mitochondrial matrix, where its escape is limited, leading to oxidative stress when its concentration exceeds the capacity of mitochondrial antioxidant defenses [33–35]. As stallion spermatozoa rely on OXPHOS over glycolysis for ATP production [36], higher intracellular $O_2^{-}\cdot$ levels are expected compared to other species. Gibb et al. (2014) found a positive relationship between sperm ROS production and functionality in horses [37], where a high concentration of $O_2^{-}\cdot$ could then be attributed to increased sperm metabolism. However, in our study, the reduced mitochondrial activity observed in live sperm from NP-treated samples suggests that the rise in $O_2^{-}\cdot$ results from altered mitochondrial function rather than elevated metabolic activity. Consistent with this, a decrease in mitochondrial membrane potential associated with a disrupted mitochondrial structure induced by MP has been reported in GC-sp [11]. Although a corresponding increase in H_2O_2 levels would also be expected due to the presence of SOD in spermatozoa, our results did not show a relationship between the increase of intracellular $O_2^{-}\cdot$ and H_2O_2 levels. A recent study identified catalase as a key antioxidant in equine sperm, contributing to their marked resistance to oxidative stress. Stallion sperm exhibit a high capacity to internalize H_2O_2 without compromising sperm function or DNA integrity, likely due to robust antioxidant defenses, particularly catalase activity [38], which could explain the elevated intracellular $O_2^{-}\cdot$ levels in live sperm from NP-treated samples without a concurrent increase in H_2O_2. Aligned with

Table 1
Effect of NP supplementation on stallion spermatozoa kinetic parameters analyzed by CASA system.

		TM	PM	VCL	VAP	VSL	STR	LIN
T0	**CTR**	28.4 ± 1.9	13.1 ± 1.3	278.6 ± 9.8	154.4 ± 5.6	101.8 ± 4.6	35.7 ± 0.9	63.14 ± 1.0
T1	**CTR**	13.4 ± 1.5 ^{a}	5.4 ± 0.8 ^{a}	269.5 ± 7.5	146.5 ± 4.8	80.7 ± 4.6	56.2 ± 1.6	30.1 ± 1.1
	10NP	13.6 ± 1.2 ^{a}	4.8 ± 0.6 ^{ab}	278.7 ± 5.8	151.4 ± 3.5	80.1 ± 3.8	53.8 ± 1.0	28.6 ± 0.7
	50NP	13.4 ± 1.7 ^{a}	5.0 ± 0.9 ^{ab}	281.5 ± 7.2	153.5 ± 4.5	83.2 ± 4.5	54.9 ± 1.0	29.4 ± 0.9
	100NP	11.0 ± 1.2 ^{ab}	4.4 ± 0.8 ^{ab}	281.0 ± 7.5	155.0 ± 5.1	82.9 ± 3.5	54.9 ± 1.5	29.5 ± 0.9
	200NP	8.8 ± 1.6 ^{b}	3.4 ± 0.7 ^{b}	294.2 ± 7.5	163.6 ± 4.7	78.6 ± 4.4	51.8 ± 1.8	27.8 ± 1.1
T3	**CTR**	3.4 ± 0.5	1.1 ± 0.2	288.9 ± 7.9	170.9 ± 5.7	53.9 ± 3.1 ^{a}	44.6 ± 1.3 ^{a}	23.1 ± 1.0 ^{a}
	10NP	3.5 ± 0.6	1.2 ± 0.3	281.9 ± 9.4	169.4 ± 6.8	51.1 ± 3.7 ^{a}	44.0 ± 2.5 ^{a}	22.9 ± 1.6 ^{a}
	50NP	3.0 ± 0.6	1.1 ± 0.2	285.0 ± 9.4	170.2 ± 6.8	53.2 ± 3.6 ^{a}	43.7 ± 2.3 ^{a}	22.7 ± 1.4 ^{a}
	100NP	2.3 ± 0.5	0.7 ± 0.2	279.4 ± 21.8	168.9 ± 13.9	47.4 ± 4.7 ^{a}	39.0 ± 3.1 ^{a}	20.8 ± 1.8 ^{a}
	200NP	1.1 ± 0.3	0.2 ± 0.1	279.8 ± 38.2	179.3 ± 24.8	34.9 ± 6.1 ^{b}	23.6 ± 3.8 ^{b}	12.8 ± 2.1 ^{b}

Percent of total motile sperm (TM), percent of progressive sperm (PM), curvilinear velocity (VCL), mean velocity (VAP), straight-line velocity (VSL), linearity (LIN), and straightness (STR). Control sample (CTR) was analyzed post-thawing (T0) and after 1 (T1) and 3 h (T3) of incubation at 38 °C, and samples supplemented with different concentration of NP (10 μg/mL or 10NP, 50 μg/mL or 50NP, 100 μg/mL or 100NP, and 200 μg/mL or 2000NP) were analyzed at T1 and T3. Data are reported as mean ± SEM (n = 15). Different letters indicate a significant difference between samples at the same time ($p < 0.05$).

this, Giaretta et al. (2022) reported no significant differences in H_2O_2 production between viable stallion spermatozoa with functional or compromised mitochondria [39]. On the other hand, no differences of H_2O_2 levels could be attributed to altered SOD activity. A recent molecular docking study reported that NP metabolites may disrupt SOD conformation, thereby exacerbating oxidative stress [40]. Therefore, it can be inferred that NP exert toxic effects via mitochondrial accumulation, impairing their activity, and triggering ROS generation, as documented by Das [41]. Further studies are warranted to clarify their impact on antioxidant enzymes. Furthermore, excessive mitochondrial production of $O_2^{-}\cdot$ in sperm has also been linked to apoptosis [33], which may explain the reduced viability observed during incubation with NP-supplemented samples.

Lastly, our data showed that NP impaired sperm motility after 1 h of incubation, consistent with previous in vitro studies in human sperm [24] and in vivo experiments in mice [19,42]. After 3 h, only VSL, STR, and LIN were altered. However, motility values in the CTR group were also very low, likely due to centrifugation to remove cryoprotectants and prolonged incubation in a suboptimal medium. Thus, kinetic parameters at 3 h should be interpreted with caution. It is well established that preserving mitochondrial membrane potential is essential for maintaining sperm motility [36,37,39,43,44]. Based on this, it can be reasonably inferred that NP may impair mitochondrial function, an effect likely more pronounced in horses, whose sperm motility relies heavily on mitochondrial metabolism, unlike humans and mice, where glycolysis plays a more prominent role [37].

In conclusion, our study demonstrates that stallion spermatozoa can internalize NP, with marked accumulation in the post-acrosomal and mid piece regions. This internalization impairs mitochondrial activity, increases intracellular superoxide levels, induces oxidative stress, and presumably promotes apoptosis, ultimately reducing sperm motility and viability. These findings suggest that global plastic pollution may compromise male reproductive function, affecting not only spermatogenesis but also mature sperm functionality. Further studies are needed to elucidate the specific alterations in sperm antioxidants defenses and the potential impact on fertility.

CRediT authorship contribution statement

Sofia Dindo: Writing – original draft, Methodology, Formal analysis, Data curation, Conceptualization. **Laura Tovar-Pascual:** Writing – review & editing, Methodology, Data curation. **Vito Antonio Baldassarro:** Writing – review & editing, Methodology, Formal analysis, Data curation. **Diego Bucci:** Writing – review & editing, Methodology, Formal analysis. **Beatrice Mislei:** Writing – review & editing, Methodology. **Marcella Spinaci:** Writing – review & editing, Supervision, Methodology, Conceptualization. **Jose Manuel Ortiz-Rodriguez:** Writing – review & editing, Supervision, Methodology, Formal analysis, Data curation, Conceptualization.

Declaration of generative AI and AI-assisted technologies in the writing process

During the preparation of this work, we used ChatGPT as an AI-assisted tool to refine the language and clarity of our English article. Following its use, we thoroughly reviewed and edited the content to ensure accuracy and appropriateness, taking full responsibility for the final published version of the article.

Funding sources

This research did not receive any specific grant from funding agencies in the public, commercial, or not-for-profit sectors.

Declaration of interests

The authors declare that they have no known competing financial interests or personal relationships that could have appeared to influence the work reported in this paper.

Acknowledgements

The assistance of the research group's laboratory technician, Cinzia Cappannari, is warmly appreciated.

Data availability

The dataset supporting this study is available at:

Dindo, S.; Tovar-Pascual, L.; Bucci, D.; Spinaci, M.; Ortiz-Rodriguez, J. M. (2025). *Experimental data about Effects of Nanoplastics exposure in mature equine spermatozoa.* University of Bologna. https://doi.org/10.6092/unibo/amsacta/8313.

References

[1] Petersen F, Hubbart JA. The occurrence and transport of microplastics: the state of the science. Sci Total Environ 2021;758. https://doi.org/10.1016/j.scitotenv.2020.143936.
[2] Yang S, Li M, Kong RYC, Li L, Li R, Chen J, et al. Reproductive toxicity of micro- and nanoplastics. Environ Int 2023;177. https://doi.org/10.1016/j.envint.2023.108002.
[3] Pujol G, Marín-Gual L, González-Rodelas L, Álvarez-González L, Chauvigné F, Cerdà J, et al. Short-term polystyrene nanoplastic exposure alters zebrafish male and female germline and reproductive outcomes, unveiling pollutant-impacted molecular pathways. J Hazard Mater 2025;481. https://doi.org/10.1016/j.jhazmat.2024.136529.
[4] Amereh F, Babaei M, Eslami A, Fazelipour S, Rafiee M. The emerging risk of exposure to nano(micro)plastics on endocrine disturbance and reproductive toxicity: from a hypothetical scenario to a global public health challenge. Environ Pollut (Amsterdam, Neth) 2020;261. https://doi.org/10.1016/j.envpol.2020.114158.
[5] D'Angelo S, Meccariello R. Microplastics: a threat for male fertility. Int J Environ Res Publ Health 2021;18:1–11. https://doi.org/10.3390/ijerph18052392.
[6] Ali N, Katsouli J, Marczylo EL, Gant TW, Wright S, Bernardino de la Serna J. The potential impacts of micro-and-nano plastics on various organ systems in humans. EBioMedicine 2024;99. https://doi.org/10.1016/j.ebiom.2023.104901.
[7] Zhu L, Kang Y, Ma M, Wu Z, Zhang L, Hu R, et al. Tissue accumulation of microplastics and potential health risks in human. Sci Total Environ 2024;915. https://doi.org/10.1016/j.scitotenv.2024.170004.
[8] Zhao Q, Zhu L, Weng J, Jin Z, Cao Y, Jiang H, et al. Detection and characterization of microplastics in the human testis and semen. Sci Total Environ 2023;877:162713. https://doi.org/10.1016/J.SCITOTENV.2023.162713.
[9] Deng Y, Zhang Y, Lemos B, Ren H. Tissue accumulation of microplastics in mice and biomarker responses suggest widespread health risks of exposure. Sci Rep 2017;7. https://doi.org/10.1038/srep46687.
[10] Yong CQY, Valiyaveettil S, Tang BL. Toxicity of microplastics and nanoplastics in Mammalian systems. Int J Environ Res Publ Health 2020;17. https://doi.org/10.3390/ijerph17051509.
[11] Liu T, Hou B, Wang Z, Yang Y. Polystyrene microplastics induce mitochondrial damage in mouse GC-2 cells. Ecotoxicol Environ Saf 2022;237. https://doi.org/10.1016/j.ecoenv.2022.113520.
[12] Zhang Y, Yin K, Wang D, Wang Y, Lu H, Zhao H, et al. Polystyrene microplastics-induced cardiotoxicity in chickens via the ROS-driven NF-κB-NLRP3-GSDMD and AMPK-PGC-1α axes. Sci Total Environ 2022;840. https://doi.org/10.1016/j.scitotenv.2022.156727.
[13] Goodman KE, Hare JT, Khamis ZI, Hua T, Sang QXA. Exposure of human lung cells to polystyrene microplastics significantly retards cell proliferation and triggers morphological changes. Chem Res Toxicol 2021;34:1069–81. https://doi.org/10.1021/acs.chemrestox.0c00486.
[14] Xu M, Halimu G, Zhang Q, Song Y, Fu X, Li Y, et al. Internalization and toxicity: a preliminary study of effects of nanoplastic particles on human lung epithelial cell. Sci Total Environ 2019;694. https://doi.org/10.1016/j.scitotenv.2019.133794.
[15] Dong C Di, Chen CW, Chen YC, Chen HH, Lee JS, Lin CH. Polystyrene microplastic particles: in vitro pulmonary toxicity assessment. J Hazard Mater 2020;385. https://doi.org/10.1016/j.jhazmat.2019.121575.
[16] Xiao M, Li X, Zhang X, Duan X, Lin H, Liu S, et al. Assessment of cancer-related signaling pathways in responses to polystyrene nanoplastics via a kidney-testis microfluidic platform (KTP). Sci Total Environ 2023;857. https://doi.org/10.1016/j.scitotenv.2022.159306.
[17] Li B, Ding Y, Cheng X, Sheng D, Xu Z, Rong Q, et al. Polyethylene microplastics affect the distribution of gut microbiota and inflammation development in mice. Chemosphere 2020;244. https://doi.org/10.1016/j.chemosphere.2019.125492.
[18] Huang W, Yin H, Yang Y, Jin L, Lu G, Dang Z. Influence of the co-exposure of microplastics and tetrabromobisphenol A on human gut: simulation in vitro with

human cell Caco-2 and gut microbiota. Sci Total Environ 2021;778. https://doi.org/10.1016/j.scitotenv.2021.146264.
[19] Jin H, Ma T, Sha X, Liu Z, Zhou Y, Meng X, et al. Polystyrene microplastics induced male reproductive toxicity in mice. J Hazard Mater 2021;401. https://doi.org/10.1016/j.jhazmat.2020.123430.
[20] Hou B, Wang F, Liu T, Wang Z. Reproductive toxicity of polystyrene microplastics: in vivo experimental study on testicular toxicity in mice. J Hazard Mater 2021;405. https://doi.org/10.1016/j.jhazmat.2020.124028.
[21] Hong Y, Wu S, Wei G. Adverse effects of microplastics and nanoplastics on the reproductive system: a comprehensive review of fertility and potential harmful interactions. Sci Total Environ 2023;903. https://doi.org/10.1016/j.scitotenv.2023.166258.
[22] Gao L, Xiong X, Chen C, Luo P, Li J, Gao X, et al. The male reproductive toxicity after nanoplastics and microplastics exposure: sperm quality and changes of different cells in testis. Ecotoxicol Environ Saf 2023;267. https://doi.org/10.1016/j.ecoenv.2023.115618.
[23] Hu CJ, Garcia MA, Nihart A, Liu R, Yin L, Adolphi N, et al. Microplastic presence in dog and human testis and its potential association with sperm count and weights of testis and epididymis. Toxicol Sci 2024;200:235–40. https://doi.org/10.1093/toxsci/kfae060.
[24] Contino M, Ferruggia G, Indelicato S, Pecoraro R, Scalisi EM, Bracchitta G, et al. In vitro nano-polystyrene toxicity: metabolic dysfunctions and cytoprotective responses of human spermatozoa. Biology 2023;12. https://doi.org/10.3390/biology12040624.
[25] Barbara M, Volsa AM, Tovar L, Gaiani M, Gugole PM, Attolini E, et al. Effects of polystyrene nanoparticles on bovine oocyte in vitro maturation. Theriogenology 2025;244:117482. https://doi.org/10.1016/J.THERIOGENOLOGY.2025.117482.
[26] Okoffo ED, Thomas KV. Quantitative analysis of nanoplastics in environmental and potable waters by pyrolysis-gas chromatography–mass spectrometry. J Hazard Mater 2024;464:133013. https://doi.org/10.1016/J.JHAZMAT.2023.133013.
[27] Fu X, Han H, Yang H, Xu B, Dai W, Liu L, et al. Nrf 2-mediated ferroptosis of spermatogenic cells involved in male reproductive toxicity induced by polystyrene nanoplastics in mice. J Zhejiang Univ - Sci B 2024;25:307–23. https://doi.org/10.1631/jzus.B2300138.
[28] Kuhn DA, Vanhecke D, Michen B, Blank F, Gehr P, Petri-Fink A, et al. Different endocytotic uptake mechanisms for nanoparticles in epithelial cells and macrophages. Beilstein J Nanotechnol 2014;5:1625–36. https://doi.org/10.3762/bjnano.5.174.
[29] Liu L, Xu K, Zhang B, Ye Y, Zhang Q, Jiang W. Cellular internalization and release of polystyrene microplastics and nanoplastics. Sci Total Environ 2021;779. https://doi.org/10.1016/j.scitotenv.2021.146523.
[30] Li S, Ma Y, Ye S, Su Y, Hu D, Xiao F. Endogenous hydrogen sulfide counteracts polystyrene nanoplastics-induced mitochondrial apoptosis and excessive autophagy via regulating Nrf2 and PGC-1α signaling pathway in mouse spermatocyte-derived GC-2spd(ts) cells. Food Chem Toxicol 2022;164. https://doi.org/10.1016/j.fct.2022.113071.
[31] Bucci D, Spinaci M, Bustamante-Filho IC, Nesci S. The sperm mitochondria: clues and challenges. Anim Reprod 2022;19. https://doi.org/10.1590/1984-3143-AR2022-0131.
[32] Karim A, Yadav A, Sweety UH, Kumar J, Delgado SA, Hernandez JA, et al. Interfacial interactions between nanoplastics and biological systems: toward an atomic and molecular understanding of plastics-driven biological dyshomeostasis. ACS Appl Mater Interfaces 2024;16:25740–56. https://doi.org/10.1021/acsami.4c03008.
[33] Aitken RJ, Whiting S, De Iuliis GN, McClymont S, Mitchell LA, Baker MA. Electrophilic aldehydes generated by sperm metabolism activate mitochondrial reactive oxygen species generation and apoptosis by targeting succinate dehydrogenase. J Biol Chem 2012;287. https://doi.org/10.1074/jbc.M112.366690.
[34] Balaban RS, Nemoto S, Finkel T. Mitochondria, oxidants, and aging. Cell 2005;120. https://doi.org/10.1016/j.cell.2005.02.001.
[35] Castellini C, D'andrea S, Cordeschi G, Totaro M, Parisi A, Di Emidio G, et al. Pathophysiology of mitochondrial dysfunction in human spermatozoa: focus on energetic metabolism, oxidative stress and apoptosis. Antioxidants 2021;10. https://doi.org/10.3390/antiox10050695.
[36] Ortiz-Rodriguez JM, Bucci D, Tovar-Pascual L, Granata S, Spinaci M, Nesci S. Analysis of stallion spermatozoa metabolism using Agilent Seahorse XFp technology. Anim Reprod Sci 2024;271. https://doi.org/10.1016/j.anireprosci.2024.107633.
[37] Gibb Z, Lambourne SR, Aitken RJ. The paradoxical relationship between stallion fertility and oxidative stress. Biol Reprod 2014;91. https://doi.org/10.1095/biolreprod.114.118539.
[38] Medica AJ, Swegen A, Seifi-Jamadi A, McIntosh K, Gibb Z. Catalase in unexpected places: revisiting H2O2 detoxification pathways in stallion spermatozoa. Antioxidants 2025;14:718. https://doi.org/10.3390/antiox14060718.
[39] Giaretta E, Mislei B, Martínez-Pastor F, Nesci S, Spinaci M, Galeati G, et al. Use of specific mitochondrial complex inhibitors to investigate mitochondrial involvement on horse sperm motility and ROS production. Res Vet Sci 2022;147:12–9. https://doi.org/10.1016/j.rvsc.2022.03.017.
[40] Fan X, Gu C, Shen L, Gao Z, Yang X, Bian Y, et al. Theoretical insights into the binding of mono/di-ethyl phthalates to superoxide dismutase and associated structural changes impairing antioxidant activity: a coupled molecular docking and dynamics simulation approach. Sci Total Environ 2025;983:179667. https://doi.org/10.1016/j.scitotenv.2025.179667.
[41] Das A. The emerging role of microplastics in systemic toxicity: involvement of reactive oxygen species (ROS). Sci Total Environ 2023;895. https://doi.org/10.1016/j.scitotenv.2023.165076.
[42] Liu Y, Hao F, Liang H, Liu W, Guo Y. Exposure to polystyrene nanoplastics impairs sperm metabolism and pre-implantation embryo development in mice. Front Cell Dev Biol 2025;13. https://doi.org/10.3389/fcell.2025.1562331.
[43] Davila MP, Muñoz PM, Bolaños JMG, Stout TAE, Gadella BM, Tapia JA, et al. Mitochondrial ATP is required for the maintenance of membrane integrity in stallion spermatozoa, whereas motility requires both glycolysis and oxidative phosphorylation. Reproduction 2016;152:683–94. https://doi.org/10.1530/REP-16-0409.
[44] Pena FJ, Oflaherty C, Ortiz Rodriguez JM, Martin Cano FE, Gaitskell-Phillips G, Gil MC, et al. The stallion spermatozoa: a valuable model to help understand the interplay between metabolism and redox (de)regulation in sperm cells. Antioxidants Redox Signal 2022;37:521–37. https://doi.org/10.1089/ars.2021.0092.